Marine Pollution Bulletin 181 (2022) 113895

Contents lists available at ScienceDirect

Marine Pollution Bulletin

journal homepage: www.elsevier.com/locate/marpolbul

Development of a gamma ray dose rate calculation and mapping tool for Lagrangian marine nuclear emergency response models

Andrew Little [a,b,*], Matthew D. Piggott [b], Andrew G. Buchan [c]

[a] Ministry of Defence, HMS Sultan, Military Road, Gosport PO12 3BY, UK
[b] Department of Earth Science and Engineering, Imperial College London, South Kensington Campus, London SW7 2AZ, UK
[c] School of Engineering and Materials Science, Queen Mary University of London, London E1 4NS, UK

ARTICLE INFO

Keywords:
Nuclear emergency response
Gamma ray dose rate
Air attenuation
Buildup
Radionuclide impact assessment
Marine release
Lagrangian model

ABSTRACT

This paper presents the development and testing of a gamma radiation dose rate calculation model for the marine environment, and evaluates the potential use for such a model in both short term nuclear emergency response management and emergency response planning. This is believed to be the first implementation of a full field gamma radiation mapping model (including air attenuation and buildup) to be incorporated within a Lagrangian marine dispersion model. Calculated surface gamma ray dose rates for nine generic release scenarios are presented and used to undertake an emergency countermeasure optioneering assessment.

1. Introduction

This paper presents the development and testing of a gamma radiation dose rate model for the marine environment, and evaluates the potential use for such a model in both short term nuclear emergency response management and emergency response planning. In particular the use of this model to undertake a cost-benefit analysis for the use of a spray drench is presented. Spray drench is a postulated nuclear emergency response countermeasure – designed to increase the atmospheric removal rate of radionuclides released from a casualty nuclear plant by spraying a continuous mist of water over the release site. This will have the effect of reducing radiation doses from atmospheric pathways; however, it comes at the cost of increasing radiation dose rates in the marine environment.

The presented model is designed to be highly adaptable both in terms of different source terms and dispersion models, and to be sufficiently fast such that it can be run in real time to support nuclear emergency response management.

In the unlikely event of a nuclear emergency, particularly from a facility located along coastal seas or estuaries, it is inevitable that a certain amount of radioactive material will be either directly released to the marine environment or else deposited onto the sea surface from the atmosphere. For example, analysis following the Fukushima Daiichi nuclear disaster by the United Nations Scientific Committee on the Effects of Atomic Radiation (UNSCEAR) estimate direct releases to the marine environment of 12.8–20.3 PBq and atmospheric deposition of 62–111 PBq of Iodine & Caesium isotopes (UNSCEAR, 2020).

In the early phases of a radiological release to the marine environment the dominant exposure pathway to members of the public (directly from the marine environment, excepting atmospheric dose pathways) is likely to be from direct gamma radiation, whilst in the longer term pathways such as ingestion of contaminated foodstuffs will become more significant. Models for predicting the consequences of postulated nuclear emergencies are essential tools in developing urgent protective action strategies and remain under active development around the world, both for marine and atmospheric discharges as outlined briefly below.

Many of the recent developments and challenges in the field of radioactive dispersion modelling in the marine environment are reviewed in Periáñez et al. (2019). Most marine dispersion models presented in that work are principally interested in single nuclide concentrations or longer term dose assessment due to uptake in the biological food chain, such as is considered in Vives i Batlle et al. (2018). which presents the development of biota uptake and dose modelling post-Fukushima.

Duffa et al. (2016) details the development of a set of emergency response tools for accidental radiological contamination of the French coast using the STERNE simulation tool. Dose assessments are not

* Corresponding author at: Ministry of Defence, HMS Sultan, Military Road, Gosport PO12 3BY, UK.
E-mail address: A.Little14@imperial.ac.uk (A. Little).

https://doi.org/10.1016/j.marpolbul.2022.113895
Received 14 January 2022; Received in revised form 1 May 2022; Accepted 8 May 2022
Available online 8 July 2022

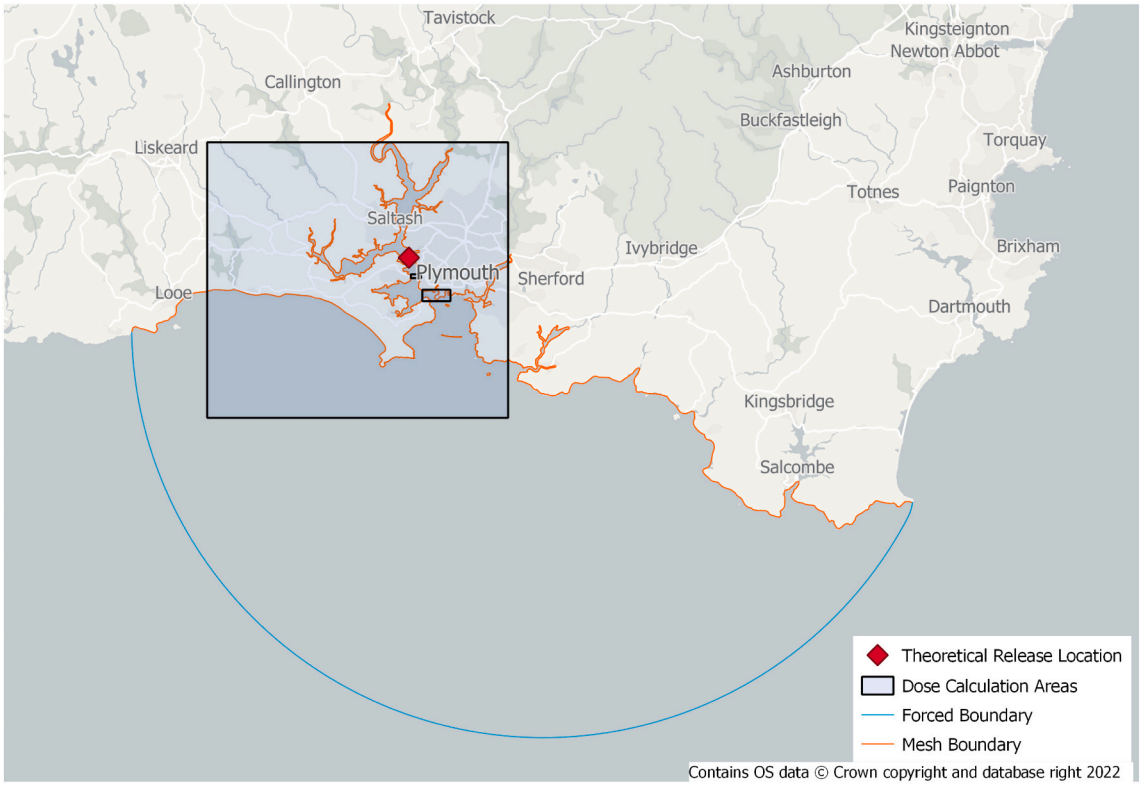

Fig. 1. Map of modelled domain showing hydrodynamic mesh extents, theoretical release location and dose calculation areas.

computed within the STERNE tool, but can be calculated using post processing tools based on calculated sea-water and marine organism concentrations. Exact details of these post processing tools are not provided, but given the model outputs concentration in seawater and biota compartments it is likely to be based on a doserate conversion factor such as presented in Kocher (1979).

Kawamura et al. (2020) presents the continued development of a Short-Term Emergency Assessment system of the Marine Environmental Radioactivity (STEAMER) developed at the Japanese Atomic Energy Agency. STEAMER is predominately focused on Cs-137 dispersion on an oceanic scale, although downscaled coastal simulations have been performed with this tool as presented in Kamidaira et al. (2019). STEAMER has also been coupled with the World-wide version of the System for Prediction of Environmental Emergency Dose Information version II (WSPEEDI-II) atmospheric model to calculate marine concentrations from deposited material as described in Kobayashi et al. (2017). Whilst WSPEEDI-II is a dose assessment tool, marine results from this work were all presented in terms of activity concentration in seawater rather than dose assessments.

Suh et al. (2021) presents the development of a similar dose assessment tool framework, RAPS-K, to assess atmospheric and marine dispersion along with dose assessment tools. The marine model used in this tool is a regional sea scale model and outputs concentrations in water, suspended sediment and bottom sediment. From the description given in this paper it is believed that only ingestion doses are calculated for the marine domain within this model framework. A groundshine dose estimate is calculated for atmospheric dispersion but it is not specified that ambient gamma dose rates were calculated for the marine domain.

Where the work of this current paper differs from the above is in the interpolation of gamma dose rates over a domain. In particular, the integration of air and water attenuation and buildup factors in a full field dose assessment is believed to be unique within a marine dispersion model. The model presented in this paper is quick-running so as to support emergency decision making in the early phases of a nuclear emergency scenario and, coupled with suitable Geo-graphic Information System (GIS) data, can provide emergency decision makers with a graphical representation of the hazard locations and magnitude across the simulation time frame. The tool can additionally be used to integrate dose rates, calculating a total dose accrued over an area of interest and time frame. This functionality allows decision makers to compare exposures with dose limits and decision criteria or to visualise such concepts as stay times.

The importance of this result interpretation for non-experts should not be understated; our tool is essential for enabling decision makers to contextualise an unfamiliar hazard that is rapidly changing both spatially and temporally. An example of such a decision making support tool is presented for atmospheric releases in Raja Shekhar et al. (2020).

Additionally, one area of increasing research interest (principally in the field of atmospheric release assessment) has been the development and use of data assimilation techniques to better estimate source terms through use of gamma dose rate measurements such as reported in Rojas-Palma et al. (2003); Zhang et al. (2017).

The gamma dose rate mapping techniques presented in this paper may allow data assimilation techniques such as these to be used for marine releases, improving longer term risk assessments by more accurately characterising the source term. Additionally, by enabling the estimation of on-land dose rates from marine releases a wider array of monitoring resources can be leveraged for data assimilation as typically more data will be available on land than from at sea monitoring due to simple logistical constraints.

2. Gamma dose rate model development

The dose assessment tool presented here has been developed using the Python firedrake[1] environment (Balay et al., 2019, 1997; Dalcin et al., 2011; Rathgeber et al., 2016) based on the output of a Lagrangian

[1] Built and tested on Firedrake release *Firedrake 20211105.0.*

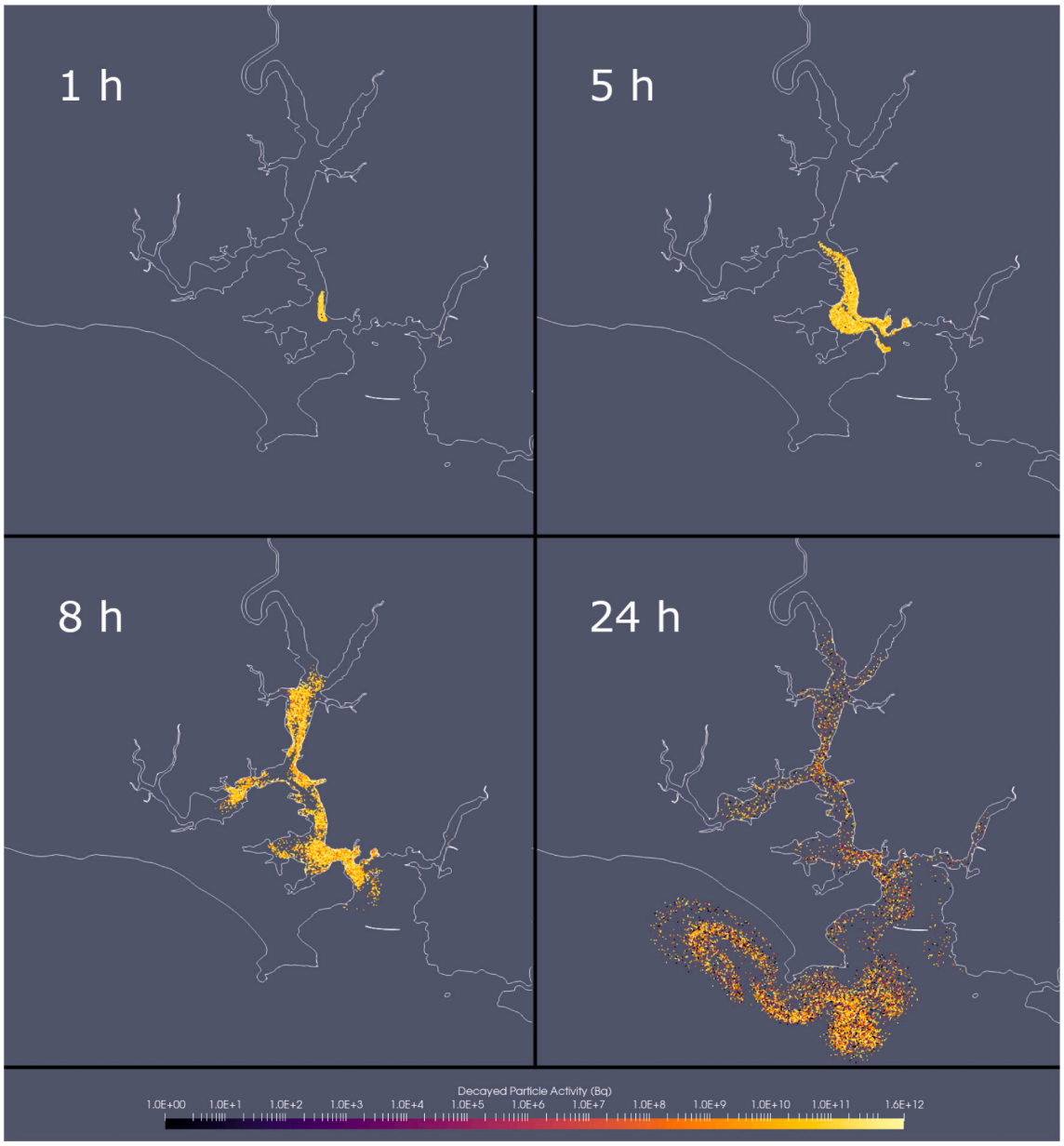

Fig. 2. Lagrangian particle model output positions for 1000 particles at various times after release. Particle colouring represents the decayed particle activity (Bq) for a release of 24 different isotopes from the WASH 1400 inventory.

particle dispersion model. Gamma dose rates are calculated for each particle and interpolated over a dose calculation spatial mesh. This mesh can either be fixed over a region of interest to allow for inter-comparison between time steps or else be set dynamically based on particle positions as the model runs. A regular 2D rectangular mesh has been used to calculate the dose rate results presented in this paper but the technique can equally be applied to unstructured or even 3D meshes.

2.1. Hydrodynamic and particle model

The results presented in this study were generated using a 2D depth averaged tidal model of the Tamar estuary (located in Plymouth, south-west England) incorporating wetting and drying which was developed using the Thetis project (Kärnä et al., 2018) – an unstructured mesh coastal ocean model, also built using the Firedrake finite element framework referenced earlier. Similar models developed in the Thetis framework for tidal applications are presented in Angeloudis et al. (2018); Vouriot et al. (2019).

The Tamar estuary was chosen for this assessment as it is both an area of active hydrodynamic model development by the authors and a location where a spray drench system may be deployed in the unlikely event of a nuclear emergency at HMNB Devonport (Reed et al., 1982). It should be stressed that the results presented in this paper are calculated against generic source terms and in no way represent any real-world scenarios at HMNB Devonport. A map of the considered domain is given in Fig. 1. This figure shows the extent of the forced mesh boundary, mesh coastline boundary, gamma dose rate calculation boundaries and hypothetical release location.

The hypothetical releases were all modelled for a period of 4 days from 09:15 UTC 01 Oct 2002. This time frame was chosen as it coincides with a tracer release study that was conducted in this region which is being used to validate the dispersion model performance. A paper presenting full details of the hydrodynamic and particle model development and validation against a tracer study is currently in preparation. The particle positions at various times after release are shown in Fig. 2.

For the purposes of development and testing of the gamma dose rate

model a number of dispersion model simplifications and adaptations were made in order to verify the gamma dose rate model behaviour and to allow an intercomparison of results during testing. Initially the 2D depth-averaged tidal model was used with a 2D Lagrangian dispersion model to give surface positions of particles. As the effect of water column shielding is significant for gamma dose rate assessment 3D distribution of particles was later introduced by stochastic sampling in order to develop the dose calculation tool. This unusual approach was only taken for testing and development as it enables verification of the model calculation steps and removes the inevitable stochastic variation from multiple Lagrangian simulations. Alternative approaches which will be explored in future work include both the use of fully 3D marine models and the use of 2D depth averaged models with a representative vertical velocity profile to drive a 3D Lagrangian dispersion model. During testing the particle model was used in basic form with no nuclide specific behaviour or sediment interaction considered. Radioactive decay was calculated at each time step for every particle but neglected daughter nuclide production.

These simplifications were justified for testing purposes and future model development will seek to address these simplifications. It should be stressed, however, that the techniques developed and presented in this paper are generic and applicable to a wide range of hydrodynamic and Lagrangian dispersion modelling techniques, so this simplification is readily overcome if desired. Due to the point nature of the calculation, the gamma dose rate function mapping approach presented in this paper is ideally suited to Lagrangian dispersion modelling, however, it could also be adapted for use in Eulerian models that are capable of exporting point values on a suitably fine resolution such as at mesh nodes.

To generate the hydrodynamic model bathymetry with a resolution of 1 arc-second was downloaded from OceanWise, Using EDINA Marine Digimap Service (2020). This bathymetry data set was used to extract a coastline contour for mesh generation. This both ensures that the bathymetry data and mesh naturally align, and enables the generation of a single continuous coastline entity – avoiding mesh generation issues due to unexpected shapefile artifacts. The extracted contour was labelled, compared against ordnance survey vector map high tide line data and manually adjusted as required within GIS Software to generate a high quality mesh. The mesh was generated using the QGIS tool as described in Avdis et al. (2018) with two density regions specifying mesh edge lengths of 10–100 m in the inner domain and 100–1000 m in the outer domain.

The forced boundary can be seen in Fig. 1 as a blue semi-circle. This boundary was forced using eleven tidal constituents (M2, S2, N2, K2, K1, O1, P1, Q1, M4, MS4, MN4) from the TPXO database Egbert and Erofeeva (2002). A region higher viscosity and Manning coefficient is calculated as a linear ramp within one kilometer of the forced boundary to improve model stability. In this model the Manning coefficient varies from 0.1 $m^{\frac{1}{3}}s^{-1}$ at the boundary to 0.01 $m^{\frac{1}{3}}s^{-1}$ in the interior. Similarly a higher viscosity region was calculated over this same region ranging from 1000 Pa s at the boundary to 1 Pa s in the model interior.

The model was initialised in a quiescent state so a seven day spin-up cycle was performed to allow the model to reach steady state before results were stored at 5 min intervals with a 10 s time step.

The model was tested and validated against UK tide gauge network data published by the British Oceanographic Data Centre for the year 2002 (British Oceanographic Data Centre, n.d.). Generally the model showed very good agreement with the gauge data and only a slight modification of bed Manning coefficient was required to adequately tune the model for generic use. It was deemed appropriate at this stage not to over-tune the hydrodynamic model.

The 5 min interval outputs from the tidal model were used to force the 2D Lagrangian particle dispersion model. This particle model was created using a Python module Percival (2020) which can be used to drive Lagrangian particles with VTK-based velocity data. The particle model can be run in 2D or 3D and can handle collisions with boundaries.

The particle model was run using the same 2D mesh as the hydrodynamic model. To test and verify model behaviour the first models were run with all particles on the surface of the water and no vertical diffusivity. Vertical diffusivity was later calculated offline to provide particle depths for testing using the local bathymetry depth from the hydrodynamic model as an upper diffusion limit. A horizontal diffusivity of 0.3 m^2s^{-1} and a vertical diffusivity of 0.005 m^2s^{-1} (where applicable) were used for model testing.

The source term activity was divided across the specified number of particles based on the appropriate sampling scheme (by activity, dose rate constant or both) to produce a library of particles labelled with activity, nuclide, decay constant, dose rate constant etc. Particles were sampled randomly from this library at each time step to match the release duration specified for the scenario in question. Custom particle labels, such as release time, can be specified at the point of release for results interpretation and testing if desired. Particle activity labels are updated at each step to track radioactive decay of the particle.

2.2. Release characteristics and source term

The results presented in this paper are derived from a series of generic release scenarios presented in the WASH 1400 reports (U.S. Nuclear Regulatory Commission, 1975) and as such do not represent any specific real-world scenario. Instead they are intended to demonstrate the gamma radiation dose model development and its application for response planning and management.

A series of hypothetical release inventories were derived for a nominal 1 MWe power reactor using the WASH 1400 inventory (T.J. McKenna, 1988, Table 2-3) and release fractions for nine PWR release scenarios reported in (U.S. Nuclear Regulatory Commission, 1975, Table 5-1). These source data are reproduced below for convenience in Tables 2 and 3.

To estimate a marine release from these atmospheric release data a washout fraction of 20 % has been applied to each of the source terms for the nine PWR scenarios, with the exception of noble gases. As noble gases will not be affected by spray drench and will not deposit into the marine environment these isotopes were removed from the marine source terms prior to calculation but were included in the comparative atmospheric dose models presented later. The 20 % removal rate is an estimated spray drench effectiveness based on work presented in Slinn (1984). Whilst using this generic figure is entirely suitable for the purposes of this initial model demonstration, the actual washout fraction is highly variable depending on particle size and water droplet size. As such, further sensitivity analysis based on the original reference Slinn (1984) and developments reported in papers such as Loosmore and Cederwall (2004) and Sportisse (2007) may be of benefit for detailed calculations in future.

2.3. Gamma energy calculation

The development intent for this model was to make it applicable to as wide a range of release scenarios as possible. As such, parameter data was required for a large number of radionuclides, not just those analysed in this study. To obtain isotopic energy data a Python-based tool was developed to scrape data from the IAEA LiveChart API International Atomic Energy Agency (2021).

For testing purposes an intensity weighted average gamma ray energy was calculated for each of 423 relevant isotopes using the API data tool (as per Eq. (1)). Whilst weighted average energy was used for development and testing, the methodology applied can easily be scaled to calculate contributions from discrete energy bands for each nuclide (noting of course that the additional computational cost to do so is likely to be high).

Error handling for missing data, metastable nuclides and nongamma emitters was included by default in the scraping tool to allow for future model expansion as required. Given that the typical length scale for dose

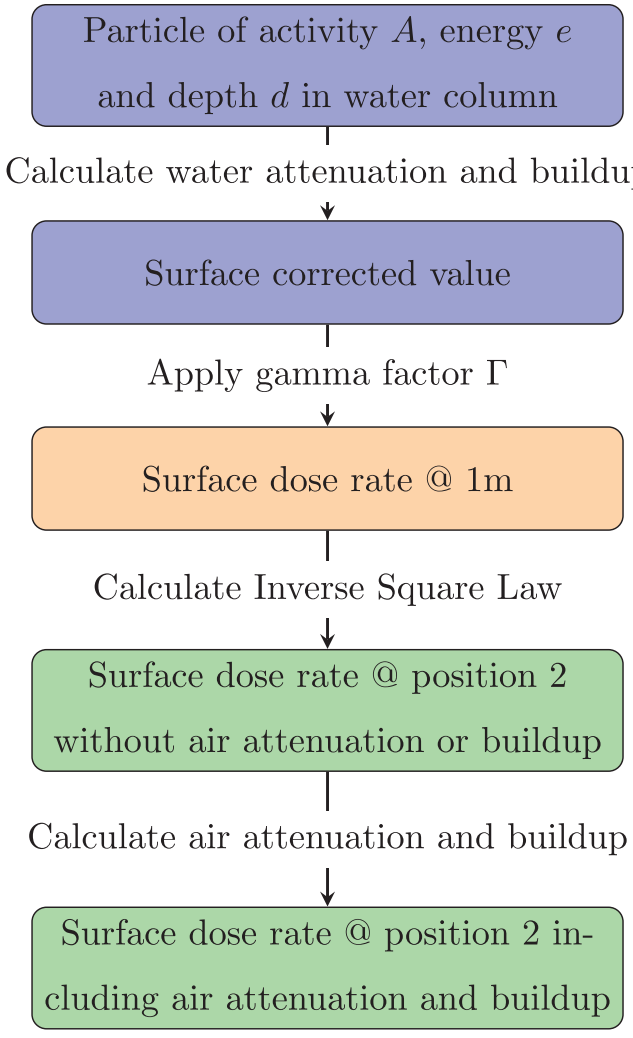

Fig. 3. Flow chart showing gamma shine calculation steps.

rate calculation in this work is several metres, beta radiation exposure has not been calculated, however, if it is desirable for other scenarios, the techniques developed here can be expanded to include beta radiation.

The intensity weighted gamma energy for each nuclide $\overline{E}$ was calculated as the sum product of the relative intensity (I_i) and energy (E_i) of each gamma ray level (i of n) divided by the sum of the intensities:

$$\overline{E} = \frac{\sum_{i=1}^{n} I_i E_i}{\sum_{i=1}^{n} I_i}. \quad (1)$$

2.4. Gamma dose rate calculation

The general layout of the model calculation steps for each particle is as outlined in Fig. 3.

The source dose rate at 1 m in air was calculated using gamma factors Γ ($mSvh^{-1}$ per MBq) taken from Unger and Trubey (1982).

The principle reduction in gamma radiation intensity in air is due to the inverse square law which describes the reduction in dose rate across the domain as follows:

$$D_1 r_1^2 = D_2 r_2^2, \quad (2)$$

where:

D_1 = The dose rate at point 1 ($mSvh^{-1}$)

r_1 = The distance to point 1 from the source (m)

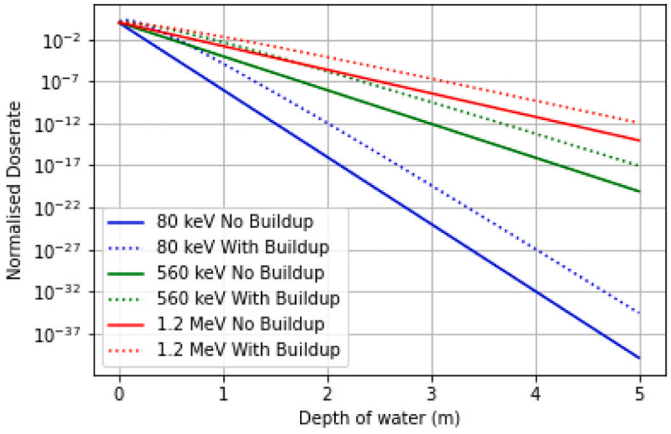

Fig. 4. Comparison of normalised dose rates with and without buildup for the maximum, mean and minimum gamma energies used in this calculation.

D_2 = The dose rate at point 2 ($mSvh^{-1}$)

r_2 = The distance (in m) to point 2 (co-ordinates (x, y)) from the source (co-ordinates (x_0, y_0)) $\equiv \sqrt{(x-x_0)^2 + (y-y_0)^2}$

Attenuation of gamma energy in water and air is calculated using the general shielding Eq. (3):

$$I(x,y) = BI_0 e^{-\frac{\mu}{\rho}\rho t}, \quad (3)$$

where: $I(x,y)$ is the intensity/dose rate at location (x,y), B is the buildup factor, I_0 is the initial intensity/dose rate, μ/ρ is the mass attenuation coefficient for the relevant material (cm^2g^{-1}), ρ is the material density (gcm^{-3}), and t is the thickness of material (cm). For water this would be the particle depth and for air this would be equivalent to r_2 as above.

Air and water mass attenuation coefficients used in this study were taken from National Institute of Standards and Technology (NIST) Data available at (U.S. National Institute of Standards and Technology, a) and (U.S. National Institute of Standards and Technology, b).

Given that intensity I and dose rate D can be considered functionally equivalent in this example and that $t \equiv r_2$, we can rearrange and simplify Eqs. (2) and (3) to generate the relation

$$D(xy) = \frac{BD_1 e^{-\frac{\mu}{\rho}\rho r_2}}{r_2^2}, \quad (4)$$

providing that D_1 is calculated at 1 m.

The *buildup* parameter, B, in Eqs. (3) and (4) represents the additional dose expected at a point within a shield due to the addition of scattered radiation. This buildup factor is dependent upon the number of mean free paths μt and the gamma energy under consideration. For large shielding thicknesses buildup significantly increases dose rates as can be seen in Fig. 4.

As the calculation distances can be large in this simulation, buildup data is required to cover a significant range of mean free paths in both water and air. Data and formula for generating buildup factors up to 40 mean free paths is presented in Trubey and Harima (1986). This technique has been expanded to 100 mean free paths by Brar et al. (1994) and these equations are presented below:

$$B(E,x) = 1 + (b-1)\frac{K^x - 1}{K - 1} \text{ for } K \neq 1, \quad (5)$$

$$B(E,x) = 1 + (b-1)x \text{ for } K = 1, \quad (6)$$

$$K(E,x) = cx^a + d \times \frac{tanh\left(\frac{x}{X_k - 2}\right) - tanh(-2)}{1 - tanh(-2)} \text{ for } x \leq 40, \quad (7)$$

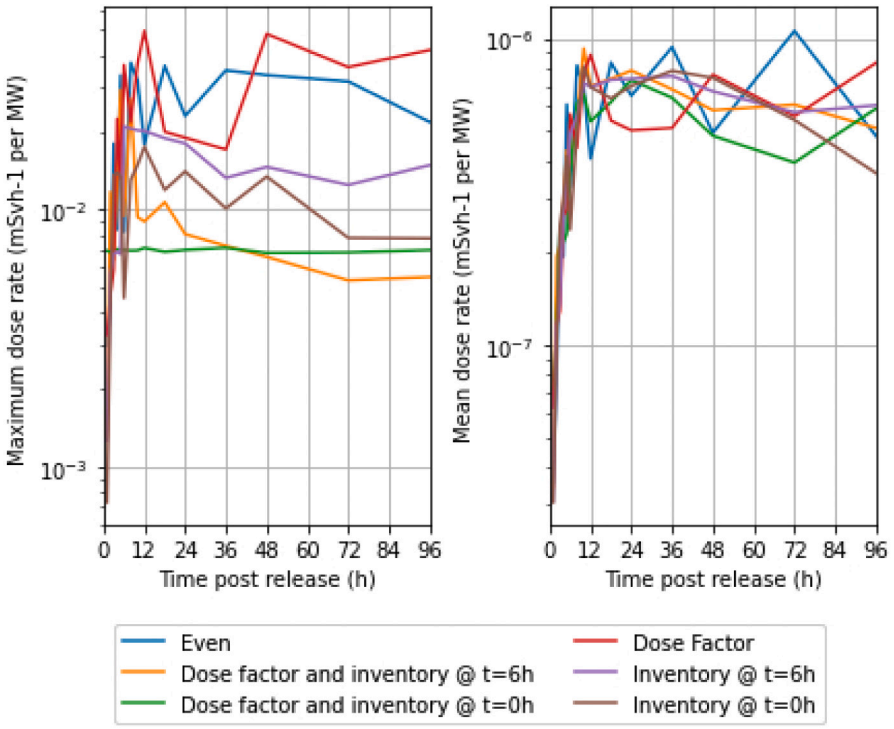

Fig. 5. Maximum and average dose rates across the domain for PWR 7 scenario and various weighting options.

$$K(E,x) = 1 + [K(35) - 1] \times exp\left[\frac{1 - \left(\frac{x}{35}\right)^{0.1}}{1 - \left(\frac{40}{35}\right)^{0.1}} ln \frac{K(40) - 1}{K(35) - 1}\right] \text{for} x > 40, \quad (8)$$

where x is the source-point distance *expressed in mean free paths* and a, b, c, d and X_k are energy-shield dependent parameters. $K(30)$ and $K(40)$ are values of K calculated using Eq. (7) at 30 and 40 mean free paths respectively.

Buildup factors for both air and water were calculated using the above formula and validated against the plots provided in Brar et al. (1994), with good agreement seen between the calculated and published values.

To maintain the generic applicability of this model, the buildup factor was calculated at run time for each particle based on particle energy. Whilst this computational overhead was not significant, for bounded scenarios a computational efficiency could be made by pre-computing these values and then using a lookup system.

The dose rates calculated for each particle are summed across the domain and saved to a pvd format output file. An option is included in the model to output dose rate contributions for each source term nuclide in addition to the total dose rate result. This feature allows the relative contributions of each nuclide to be analysed and is expected to be of significant benefit for particle models which include nuclide specific dispersion behaviour such as chemical speciation and sediment interactions.

3. Results

3.1. Model testing and verification

Basic model functionality was first verified on an idealized domain and during model development the model sensitivity to a number of factors was tested. These included the impact of the number of particles in the simulation, the mesh edge length and the inventory weighting scheme.

3.1.1. Inventory weighting scheme

Given the range of isotopes considered within this model it was considered that the means by which the source term activity was sampled across the particles in the Lagrangian dispersion model may have an influence on the results of the gamma dose rate calculation. This is due to the relative importance of the isotopes' gamma factor (initial dose rate), source term activity, and the effect of radioactive decay for short lived isotopes. Depending upon the source term sampling regime, greater or lesser bias may be applied to each of these factors, thus influencing the results of the gamma dose rate calculation.

For instance, if a large number of particles in the simulation are assigned to a short lived isotopes, these particles will become insignificant at later time steps due to decay, reducing the effective number of particles within the simulation. A number of tests were conducted to investigate the model sensitivity to this parameterisation as outlined below:

Even distribution Particles were evenly distributed across all isotopes in the inventory.

Weighted by inventory, **without decay** Particles were assigned weighted to those isotopes with the greatest activity within the source term. This activity was taken at $t0$.

Weighted by inventory, **normalised to 6 h of decay** As above but the particle weighting was calculated after 6 h of decay - this removes the influence of highly active but short-lived isotopes. Note that the particle activity was still calculated at $t0$, only the particle weighting was calculated based on six hours of decay. Six hours was chosen in this study as the mid-point of the slowest WASH1400 release scenario. The sensitivity of a specific inventory under analysis should be tested against a representative decay time for that inventory and scenario as these may be significantly different to those under test in this paper.

Weighted by gamma factor Particles were assigned weighted to those isotopes with the highest gamma factor. These are typically shorter lived isotopes.

Weighted by inventory and gamma factor, **without decay** Particles were assigned weighted by the product of source term activity and dose factor.

Weighted by inventory and gamma factor, **with 6 h of decay** As

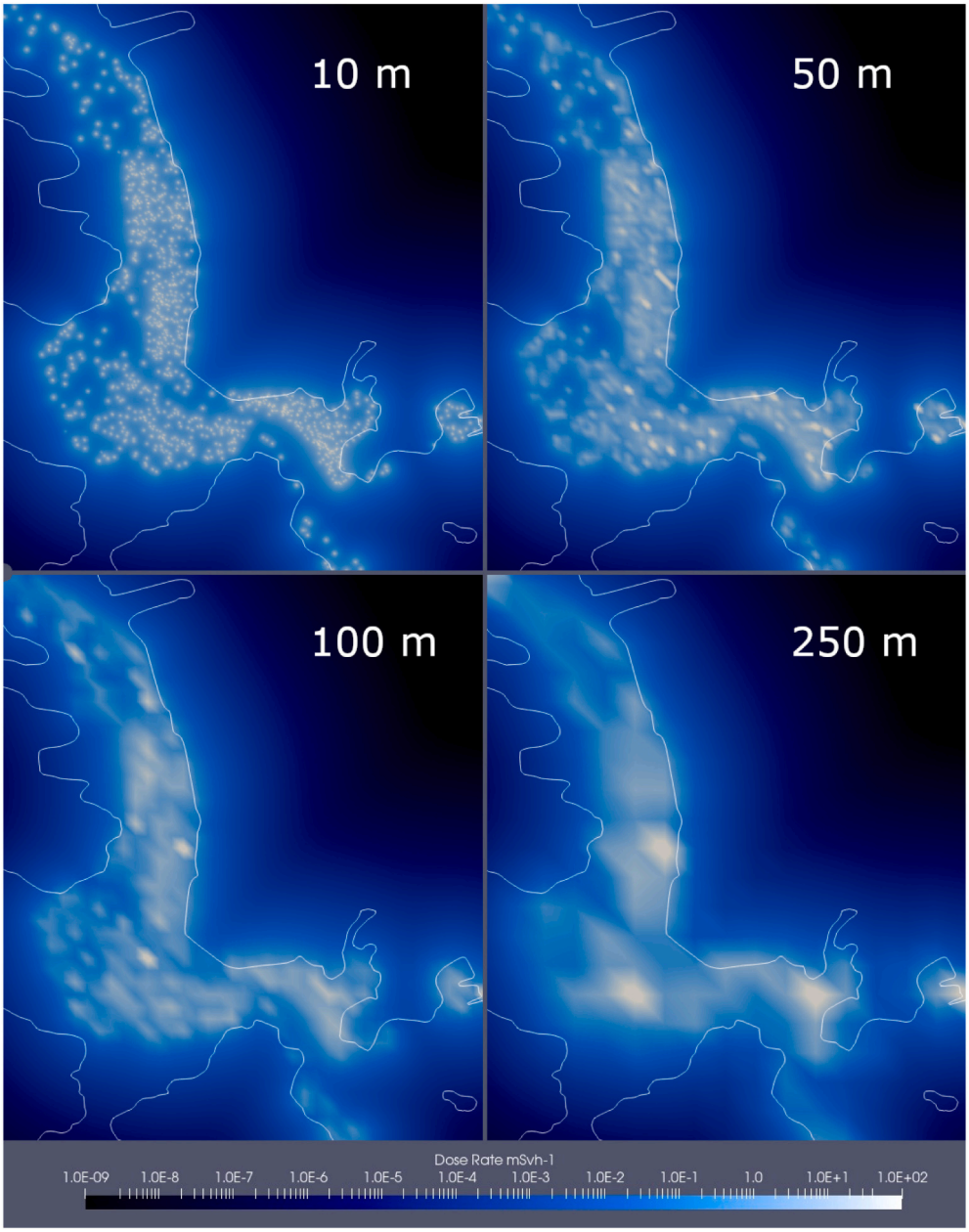

Fig. 6. Dose rate results for various mesh edge lengths. Calculated for the most extreme scenario (PWR1).

above but with the source term activity weighting decayed by 6 h.

Test results from these weighting options for the PWR 7 scenario are presented in Fig. 5. As can be seen in this figure the different weighting methods produce significant variation in the calculated maximum dose rates whilst the domain average dose rates for each scenario remain in much closer agreement. These results clearly demonstrate the requirement for using an appropriate sampling and weighting technique when initialising multi-nuclide Lagrangian models. As sampling the source term weighted by both dose factor and inventory resulted in the flattest maximum dose value profile, this weighting method was chosen for the inter-comparison work presented below. For assessing real scenarios, selection of the weighting method should be undertaken based on the desired model outputs including time frame of interest and desired degree of pessimism within the calculation.

3.1.2. Mesh edge length

Selecting the correct mesh element size for the dose calculation requires a balance between computational efficiency and result fidelity. At large mesh elements visual results will be blurry and quantitative results for average dose rate may be over-estimated. To assess the necessary mesh sizing to achieve stable results a series of mesh size comparisons were undertaken using the PWR 1 release scenario at 5 h. The results are presented below in Fig. 6. Although all of these results exhibit similar behaviour in the mid and far field dose rates, the under-sampling of the estuary is clearly visible at 250 m and to a lesser extent at 100 m. Whilst reducing the mesh edge length from 50 to 10 m results in a further improvement in resolution, the associated computational cost was deemed unjustified and 50 m mesh edge lengths were used for the remainder of the simulations presented in this work.

3.1.3. Number of particles in simulation

A truncated sensitivity study was undertaken to assess the impact that the number of particles had on the predicted dose rate and to estimate a minimum number of particles for results convergence to occur.

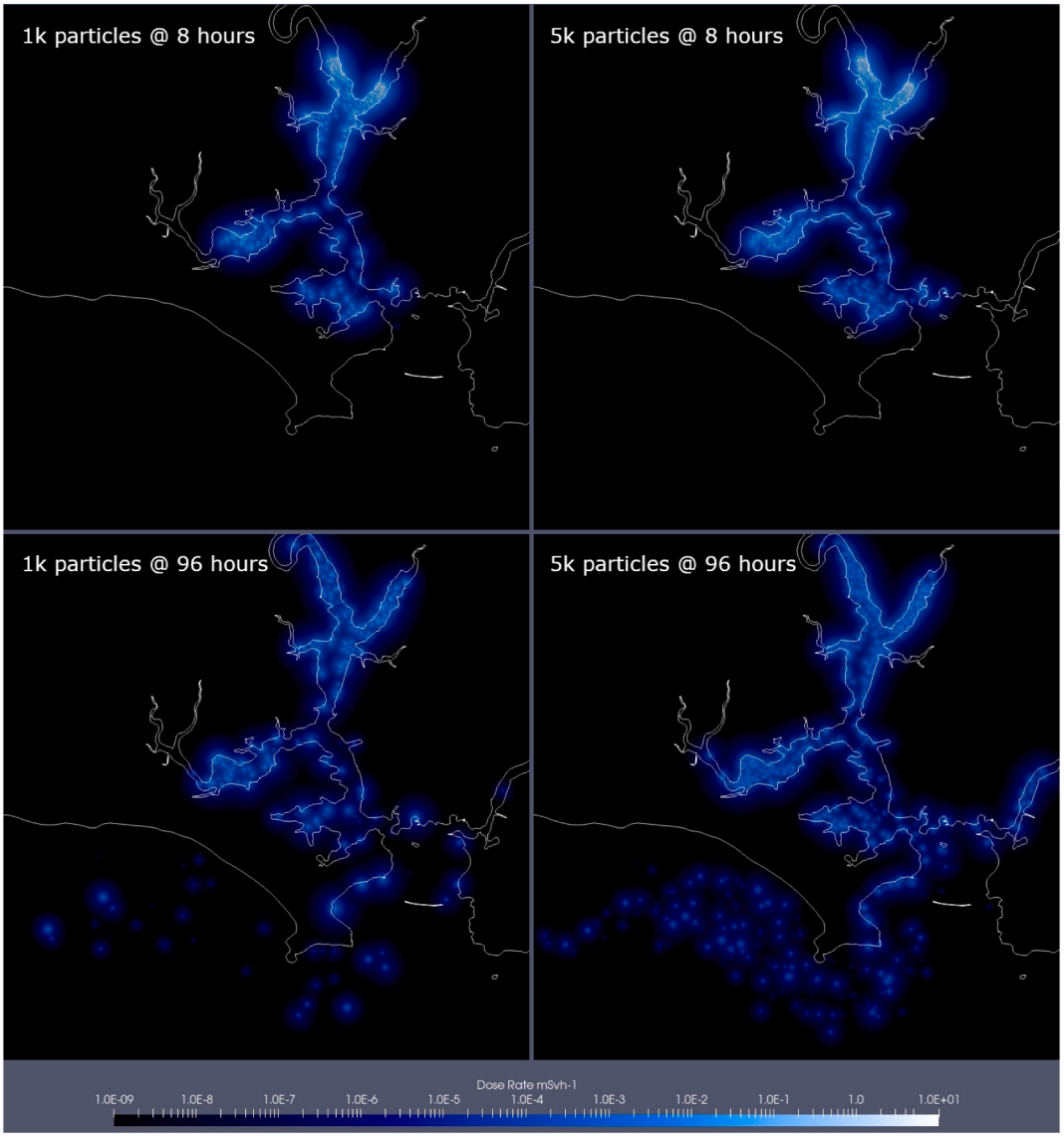

Fig. 7. Dose rate plots for 1000 and 5000 particles for 8 and 96 h endpoints.

As with the mesh edge length assessment, there is a balance to be struck between computational efficiency and resolution.

This initial scoping study found limited differences in calculated dose rates for 1000 and 5000 simulated particles with variances of average dose rate across the entire domain within 17 %. As expected, due to clustered particles superimposing dose rates, spot maximum dose rates were an average of 68 % higher for the 5000 particle results, however this effect quickly dissipated in the medium and far field.

For time steps up to around 12 h the results for 1000 and 5000 particles remain visually very similar. After 12 h more divergence in the results becomes visible as can be seen in Fig. 7 below. The difference in results for greater time steps is partly due to the stochastic sampling of particle depth, and the associated strong water column attenuation. With a greater number of particles in the simulation there is a proportionately greater probability of still having particles in the surface layers of the model, and therefore an increased dose rate. This effect is clearly visible in the deeper water of Plymouth sound, beyond the breakwater for the results at 96 h in Fig. 7.

It was concluded that 1000 particles represented an adequate number for the purposes of this scoping study, but that greater numbers may be required for real-world assessments. Further investigation below 1000 particles was not conducted as the model calculation time was sufficiently fast at 1000 particles not to warrant further investigation. For regions of higher turbulence or over longer time periods a greater number of particles may be required within the simulation.

3.2. *General applicability of dose model to emergency response planning and management*

The results shown in Figs. 8 and 10 demonstrate the benefit of this model technique for informing decision makers of the temporally and spatially variant hazard. At a glance, any emergency responder can understand the scale and extent of the hazard, without the need for data interpretation from an expert. Understanding the nature and extent of the radiological hazard is key to making balanced decisions about the implementation of urgent protective actions and enables the targeting of radiation monitoring data collection to support decision making.

For more detailed analysis by technical experts, line data can be extracted from the mesh data such as is presented in Fig. 9. This figure presents maximum and mean dose rates for all PWR scenarios for a four day period, all using the same larger dose mesh as presented in Fig. 1 previously.

The smaller area shown in Fig. 1 was also used to analyse expected dose rates and total dose exposure to a hypothetical region of interest. In

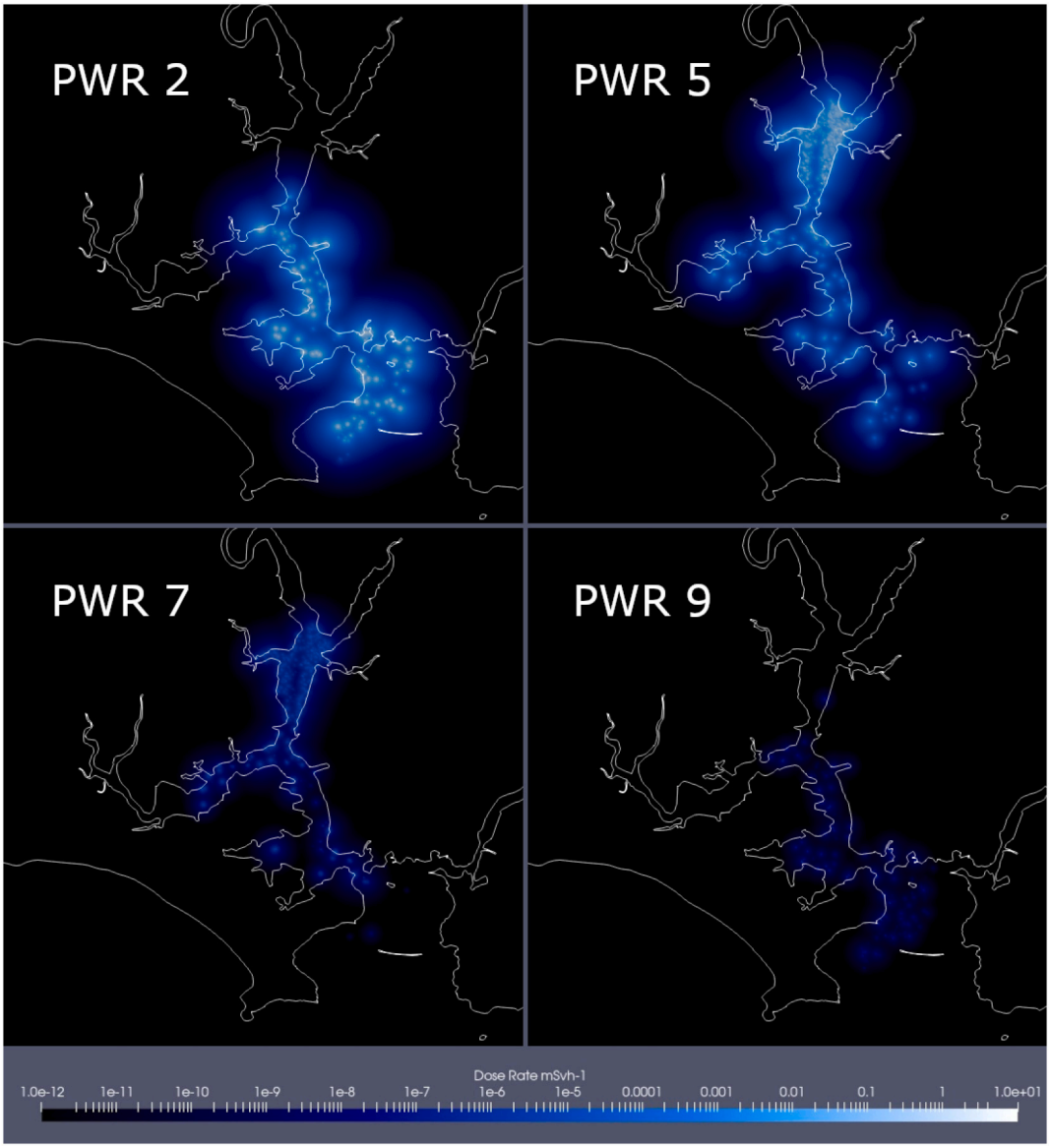

Fig. 8. Visual comparison various release scenarios, all at the same time step.

this case Fig. 10 shows the results of a dose rate integration over 6 h for a region containing a leisure marina. Understanding the extent of a gamma shine hazard in this area would be critical to making effective emergency response decisions and optimising the protection of members of the public who may, for instance, be living on board vessels in this area. The dose rate plot in Fig. 10 shows the rise and fall in dose rate as a plume of particles move through the region on the ebb tide before a second, lower peak in dose rate is seen corresponding to a more dilute plume returning through the area on the flood tide. By integrating the dose rate at this location, the time to reach a dose constraint or decision threshold can easily be calculated as shown on the graph.

The result interpretation techniques demonstrated above, whilst simple, are a very effective means of communicating radiation risk and managing emergency response actions by clearly articulating otherwise abstract concepts such as stay times and decision deadlines to nontechnical emergency response decision makers. By better understanding the nature and extent of the hazard, better decisions can be made about the appropriateness of response actions to protect members of the public.

3.3. Spray drench assessment

To assess the relative impact of spray drench on atmospheric pathway doses the National Radiological Protection Board (NRPB) W19 emergency data handbook approach (McColl and Prosser, 2002) was used to calculate centre-line doses for *plume immersion*, *inhalation* and *ground-shine* for four days at 500 m for each of the nine PWR scenarios presented above.

Four days of ground-shine exposure was chosen to match the modelled marine dispersion duration and as a pessimistic upper bound of the maximum urgent protective action implementation duration. For a typical nuclear facility 500 m approximates the distance to the site boundary and hence the distance of the most exposed member of the public. Long term impacts such as ingestion of contaminated foodstuffs were neglected for the purposes of this assessment. Whilst this is a simplistic approach, it was deemed adequate for the purposes of this comparative study.

Results for this analysis are presented in Table 1. From these results a number of conclusions can be drawn:

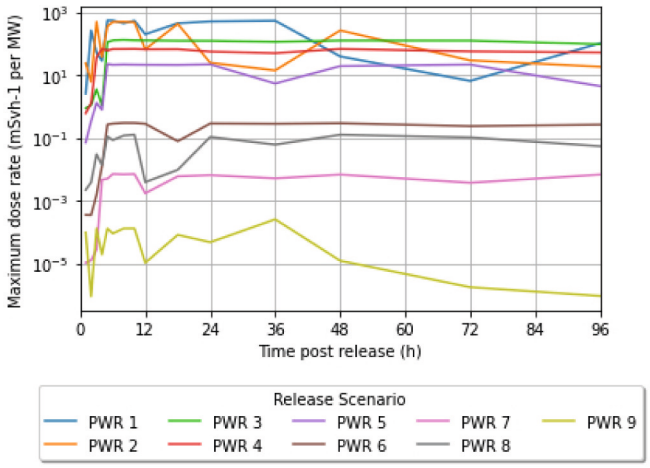

(a) Maximum dose rates calculated for all scenarios.

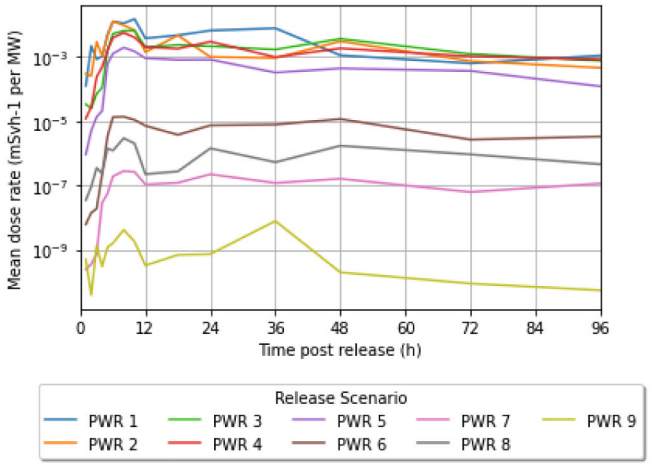

(b) Mean dose rates calculated for all scenarios

Fig. 9. Maximum and mean dose rates calculated for all scenarios.

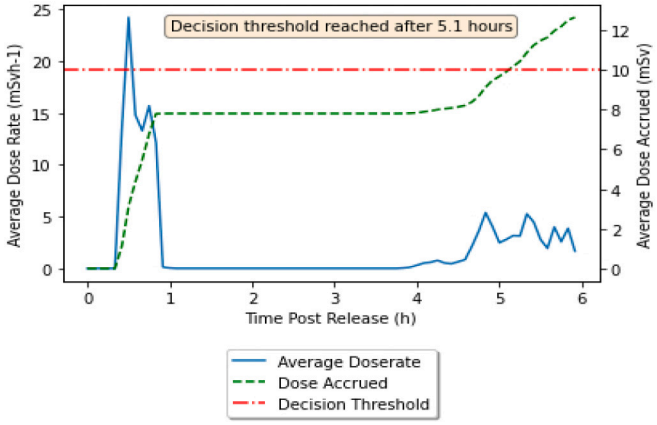

Fig. 10. Notional dose rate and total dose accrual including a response decision threshold.

- The postulated spray drench countermeasure has the potential to significantly reduce atmospheric doses
- The average increase in dose rate across the whole marine environment due to spray drench is small in comparison
- The potential maximum dose rate in the marine environment is high and therefore on an individual basis the dose saving could be outweighed should someone continue to be exposed to high radiation dose rates in the marine environment - for example someone remaining on board a leisure craft in a marina close to the release site.

Table 1
Total atmospheric dose savings with spray drench compared against increases in marine dose rates.

Scenario	Total atmospheric Dose Reduction (mSv)	Peak marine dose Rate (mSvh-1)	Average marine dose Rate (mSvh-1)
PWR 1	2.72E+02	5.45E+02	4.85E-03
PWR 2	2.02E+02	4.94E+02	3.32E-03
PWR 3	9.89E+01	1.30E+02	2.24E-03
PWR 4	1.46E+01	6.77E+01	1.81E-03
PWR 5	3.35E+00	2.21E+01	6.03E-04
PWR 6	4.73E-01	2.95E-01	5.68E-06
PWR 7	9.54E-03	6.99E-03	1.15E-07
PWR 8	2.29E-02	1.25E-01	9.21E-07
PWR 9	2.73E-05	2.52E-04	1.39E-09

As such, despite the inherent benefits of spray drench at reducing atmospheric doses, a generic statement as to the applicability of spray drench as a counter-measure cannot be given, therefore it is suggested that its use should be assessed against likely exposure scenarios as shown in Fig. 10.

This individual dose assessment will provide a justification for the emergency response countermeasure based upon the limitation principle, however, the relative impact on collective dose should also be assessed for countermeasure optimisation. Due to the low population density of water users it is expected that on a collective dose basis spray drench would always be an appropriate countermeasure to consider.

3.4. Applicability to other scenarios

Whilst the model presented above is most applicable to emergency response scenarios with associated large releases of radioactivity and therefore higher dose rates, the model is completely scalable and this can be used to analyse other radionuclide releases to the marine environment such as routine releases or accidental discharges.

4. Conclusions and further work

A versatile and functional tool for assessing the direct gamma shine doses from radioactive material releases to the marine environment has been presented, and its applicability to emergency response management demonstrated.

Due to the high shielding factor of water, the model results were found to be highly sensitive to vertical diffusion rates within the water column. Understanding this model sensitivity enables a greater focus to be placed on accurately characterising this parameter and undertaking appropriate sensitivity analysis for this factor within the dispersion model.

Whilst calculating the gamma dose rate across the full mesh extent for all particles was a robust and logical approach, it certainly not the most computationally efficient approach. Alternative approaches that could be considered include merging particle-centric fixed field distributions and truncating the interpolation distance around each particle within a main field. Similarly buildup factors for each isotope and energy could be precomputed to reduce computational overhead. At present neither of these factors are limiting as the model can run within minutes on a single core for the domain and timescales of interest, however, if there was a desire to calculate discrete rather than averaged energies for each nuclide these computational efficiencies would likely be required.

5. Data tables

Table 2
WASH1400 Core inventory (Bq) per MWe.

Isotope	Core activity (Bq)	Isotope	Core activity (Bq)
Sr	9.40E+04	131I	8.50E+04
Sr	3.70E+03	132I	1.20E+05
Sr	1.10E+05	133I	1.70E+05
Y	1.20E+05	134I	1.90E+05
Mo	1.60E+05	135I	1.50E+05
Ru	1.10E+05	134Cs	7.50E+03
Ru	2.50E+04	136Cs	3.00E+03
mTe	5.30E+03	137Cs	4.70E+03
mTe	1.30E+04	140Ba	1.60E+05
Te	1.20E+05	140La	1.60E+05
Sb	6.10E+03	144Ce	8.50E+04
Sb	3.30E+04	239Np	1.64E+06

Adapted from (T.J. McKenna, 1988, Table 2-3).

Table 3
WASH 1400 PWR Scenario release parameters.

	Time of	Duration of	Release fraction							
Scenario	Release (h)	Release (h)	Xe, Kr	Org. I	I	Cs, Rb	Te, Sb	Ba, Sr	Ru, Mo	La, Y, Ce, Np
PWR 1	2.5	0.5	9.0E-01	6.0E-03	7.0E-01	4.0E-01	4.0E-01	5.0E-02	4.0E-01	3.0E-03
PWR 2	2.5	0.5	9.0E-01	7.0E-03	7.0E-01	5.0E-01	3.0E-01	6.0E-02	2.0E-02	4.0E-03
PWR 3	5	1.5	8.0E-01	6.0E-03	2.0E-01	2.0E-01	3.0E-01	2.0E-02	3.0E-02	3.0E-03
PWR 4	2	3	6.0E-01	2.0E-03	9.0E-02	4.0E-02	3.0E-02	5.0E-03	3.0E-03	4.0E-04
PWR 5	2	4	3.0E-01	2.0E-03	3.0E-02	9.0E-03	5.0E-03	1.0E-03	6.0E-04	7.0E-05
PWR 6	12	10	3.0E-01	2.0E-03	8.0E-04	8.0E-04	1.0E-03	9.0E-05	7.0E-05	1.0E-05
PWR 7	10	10	6.0E-03	2.0E-05	2.0E-05	1.0E-05	2.0E-05	1.0E-06	1.0E-06	2.0E-07
PWR 8	0.5	0.5	2.0E-03	5.0E-06	1.0E-04	5.0E-04	1.0E-06	1.0E-08	0.0E+00	0.0E+00
PWR 9	0.5	0.5	3.0E-06	7.0E-09	1.0E-07	6.0E-07	1.0E-09	1.0E-11	0.0E+00	0.0E+00

Reproduced from (U.S. Nuclear Regulatory Commission, 1975 Table 5-1).

CRediT authorship contribution statement

Andrew Little: Conceptualization, Methodology, Software, Investigation, Writing – original draft. **Matthew D. Piggott:** Supervision, Writing – review & editing. **Andrew Buchan:** Supervision.

Declaration of competing interest

The authors declare that they have no known competing financial interests or personal relationships that could have appeared to influence the work reported in this paper.

Acknowledgements

AL is completing a PhD at Imperial College London funded by the UK Ministry of Defence. AGB wishes to acknowledge EPSRC funding through grant EP/M022684/2. MDP wished to acknowledge EPSRC funding through grant EP/R029423/1.

References

Angeloudis, A., Kramer, S.C., Avdis, A., Piggott, M.D., 2018. Optimising tidal range power plant operation. Appl. Energy 212, 680–690.
Avdis, A., Candy, A.S., Hill, J., Kramer, S.C., Piggott, M.D., 2018. Efficient unstructured mesh generation for marine renewable energy applications. Renew. Energy 116, 842–856.
Balay, S., Abhyankar, S., Adams, M.F., Brown, J., Brune, P., Buschelman, K., Dalcin, L., Eijkhout, V., Gropp, W.D., Karpeyev, D., Kaushik, D., Knepley, M.G., May, D.A., McInnes, L.C., Mills, R.T., Munson, T., Rupp, K., Sanan, P., Smith, B.F., Zampini, S., Zhang, H., Zhang, H., 2019. PETSc Users Manual. Technical Report ANL-95/11 - Revision 3.11. Argonne National Laboratory.
Balay, S., Gropp, W.D., McInnes, L.C., Smith, B.F., 1997. Efficient management of parallelism in object oriented numerical software libraries. In: Arge, E., Bruaset, A. M., Langtangen, H.P. (Eds.), Modern Software Tools in Scientific Computing. Birkhäuser Press, pp. 163–202.
Vives i Batlle, J., Aoyama, M., Bradshaw, C., Brown, J., Buesseler, K.O., Casacuberta, N., Christl, M., Duffa, C., Impens, N.R.E.N., Iosjpe, M., Masqué, P., Nishikawa, J., 2018. Marine radioecology after the fukushima dai-ichi nuclear accident: are we better positioned to understand the impact of radionuclides in marine ecosystems? Sci. Total Environ. 618, 80–92.
Brar, G.S., Singh, K., Singh, M., Mudahar, G.S., 1994. Energy absorption buildup factor studies in water, air and concrete up to 100 mfp using G-P fitting formula. Radiat. Phys. Chem. 43, 623–627.
British Oceanographic Data Centre, n.d., British Oceanographic Data Centre,. BODC Processed UK Tide Gauge Network Data.
Dalcin, L.D., Paz, R.R., Kler, P.A., Cosimo, A., 2011. Parallel distributed computing using Python. Adv. Water Resour. 34, 1124–1139. https://doi.org/10.1016/j.advwatres.2011.04.013 new Computational Methods and Software Tools.
Duffa, C., Bailly du Bois, P., Caillaud, M., Charmasson, S., Couvez, C., Didier, D., Dumas, F., Fievet, B., Morillon, M., Renaud, P., Thébault, H., 2016. Development of emergency response tools for accidental radiological contamination of french coastal areas. J. Environ. Radioact. 151 (Pt 2), 487–494.
Egbert, G.D., Erofeeva, S.Y., 2002. Efficient inverse modeling of barotropic ocean tides. J. Atmos. Ocean. Technol. 19, 183–204.
International Atomic Energy Agency, 2021. https://nds.iaea.org/relnsd/vcharthtml/api_v0_guide.html. (Accessed 10 November 2021).
Kamidaira, Y., Kawamura, H., Kobayashi, T., Uchiyama, Y., 2019. Development of regional downscaling capability in STEAMER Ocean prediction system based on multi-nested ROMS model. J. Nucl. Sci. Technol. 56, 752–763.
Kärnä, T., Kramer, S.C., Mitchell, L., Ham, D.A., Piggott, M.D., Baptista, A.M., 2018. Thetis coastal ocean model: discontinuous galerkin discretization for the three-dimensional hydrostatic equations. Geosci. Model Dev. 11, 4359–4382.

Kawamura, H., Kamidaira, Y., Kobayashi, T., 2020. Predictability of a short-term emergency assessment system of the marine environmental radioactivity. J. Nucl. Sci. Technol. 57, 472–485.
Kobayashi, T., Kawamura, H., Fujii, K., Kamidaira, Y., 2017. Development of a short-term emergency assessment system of the marine environmental radioactivity around Japan. J. Nucl. Sci. Technol. 54, 609–616.
Kocher, D.C., 1979. Dose-rate conversion factors for external exposure to photon and electron radiation from radionuclides occurring in routine releases from nuclear fuel cycle facilities. [Conversion factors are given for dose rates to 21 organs from 240 different radionuclides for 3 different modes of exposure]. In: Technical Report NUREG/CR-0494; ORNL/NUREG/TM-283. Oak Ridge National Lab, TN (USA).
Loosmore, G.A., Cederwall, R.T., 2004. Precipitation scavenging of atmospheric aerosols for emergency response applications: testing an updated model with new real-time data. Atmos. Environ. 38, 993–1003.
McColl, N.P., Prosser, S.L., 2002. NRPB - W19 Emergency Data Handbook. Technical Report W19. National Radiological Protection Board (NRPB).
OceanWise, Using EDINA Marine Digimap Service, 2020. Marine Themes Digital Elevation Model 1 Arc Second [ASC geospatial Data], Scale 1:50000, tiles: 5050010050, 5050010045, 5050010040, 5049510050, 5049510045, 5049510040.
Percival, J., 2020. ParticleModule: A Python Module for Driving Lagrangian Particles Via vtk Formatted Data.
Periáñez, R., Bezhenar, R., Brovchenko, I., Du_a, C., Iosjpe, M., Jung, K.T., Kim, K.O., Kobayashi, T., Liptak, L., Little, A., Maderich, V., McGinnity, P., Min, B.I., Nies, H., Osvath, I., Suh, K.S., de With, G., 2019. Marine radionuclide transport modelling: recent developments, problems and challenges. Environ. Model. Softw. 122, 104523.
Raja Shekhar, S.S., Venkata Srinivas, C., Rakesh, P.T., Deepu, R., Prasada Rao, P.V.V., Baskaran, R., Venkatraman, B., 2020. Online nuclear emergency response system (ONERS) for consequence assessment and decision support in the early phase of nuclear accidents - simulations for postulated events and methodology validation. Prog. Nuclear Energy 119, 103177.
Rathgeber, F., Ham, D.A., Mitchell, L., Lange, M., Luporini, F., McRae, A.T.T., Bercea, G. T., Markall, G.R., Kelly, P.H.J., 2016. Firedrake: automating the finite element method by composing abstractions. URL: ACM Trans. 30 Math. Softw. 43 (24), 1–24. https://doi.org/10.1145/2998441, arXiv:1501.01809 http://arxiv.org/abs/1501.01809.
Reed, G.W., Witchell, R.J., Coldwell, F.M., Kelleher, J.A., Frettsome, C.A., Scott, K.F., Dawson, J.L., Hambly, E.C., Tatham, P., Giles, R.W., Evans, D., Reardon, M.J., Hattersley, D., Norris, K.B., 1982. DEVONPORT dock-yard, submarine refit complex. 8445 & 8446 discussion. Proc. Inst. Civ. Eng. 72, 393–399.
Rojas-Palma, C., Madsen, H., Gering, F., Puch, R., Turcanu, C., Astrup, P., Müller, H., Richter, K., Zheleznyak, M., Treebushny, D., Kolomeev, M., Kamaev, D., Wynn, H., 2003. Data assimilation in the decision support system rodos. Radiat. Prot. Dosim. 104, 31–40.
Slinn, W.G.N., 1984. Precipitation scavenging. In: Atmospheric Science and Power Production. Technical Report DOE/TIC-27601. USDOE Technical Information Center, Oak Ridge, TN.
Sportisse, B., 2007. A review of parameterizations for modelling dry deposition and scavenging of radionuclides. Atmos. Environ. 41, 2683–2698.
Suh, K.S., Park, K., Min, B.I., Kim, S., Kim, J., 2021. Development of a web-based radiological emergency preparedness system for nuclear accidents. Ann. Nucl. Energy 156, 108203.
T.J. McKenna, J.G.G., 1988. Source Term Estimation During Incident Response to Severe Nuclear Power Plant Accidents. Technical Report NUREG 1228. U.S. Nuclear Regulatory Commission.
Trubey, D.K., Harima, Y., 1986. New Buildup Factor Data for Point Kernel Calculations. Technical Report. Oak Ridge National Lab.
Unger, L.M., Trubey, D.K., 1982. Specific Gamma-ray Dose Constants for Nuclides Important to Dosimetry and Radiological Assessment. Technical Report ORNL/RSIC-45/R1. Oak Ridge National Laboratory.
UNSCEAR, 2020. UNSCEAR 2020 report - annex B: levels and effects of radiation exposure due to the accident at the Fukushima Daiichi Nuclear Power Station: implications of information published since the UNSCEAR 2013 report. In: Technical Report Advance Copy. United Nations Scientific Committee on the Effects of Atomic Radiation.
U.S. National Institute of Standards and Technology. a. NIST: X-Ray mass attenuation coefficients - air, dry. https://physics.nist.gov/PhysRefData/XrayMassCoef/ComTab/air.html. (Accessed 14 October 2021).
U.S. National Institute of Standards and Technology. b. NIST: X-Ray mass attenuation coefficients - water, liquid. https://physics.nist.gov/PhysRefData/XrayMassCoef/ComTab/water.html. (Accessed 14 October 2021).
U.S. Nuclear Regulatory Commission, 1975. WASH 1400 Reactor Safety Study: An Assessment of Accident Risks in U.S. Commercial Nuclear Power Plants. Technical Report NUREG-75/014. U.S. NRC.
Vouriot, C.V.M., Angeloudis, A., Kramer, S.C., Piggott, M.D., 2019. Fate of large-scale vortices in idealized tidal lagoons. Environ. Fluid Mech. 19, 329–348.
Zhang, X., Raskob, W., Landman, C., Trybushnyi, D., Li, Y., 2017. Sequential multi-nuclide emission rate estimation method based on gamma dose rate measurement for nuclear emergency management. J. Hazard. Mater. 325, 288–300.